On Pressure Mode Shapes Arising from Rotor/Stator Interactions

Gary Franke and **Richard Fisher**, Voith Siemens Hydro Power Generation Inc., York, Pennsylvania
Chris Powell, Structural Technology Corporation, Zoar, Ohio
Ulrich Seidel and **Jiri Koutnik**, Voith Siemens Hydro Power Generation GmbH & Co. KG, Heidenheim, Germany

Rotor Stator Interaction (RSI) is an important source of pressure pulsations in hydro-machinery. RSI pressure pulsations induce vibrations in both stationary and rotating components. For the first time, the time variant and spatial nature of these pressure distributions (pressure mode shapes) have been visualized. A reversible pump-turbine with 20 wicket gates was tested with runners having six and nine blades. Numerous pressure transducers located in the priming chamber, between the runner and wicket gates, and between the runner crown and head cover were recorded. These data were analyzed with ME'scopeVES from Vibrant Technology, Inc. to produce animated visualization of the pressure fields. The kinematics of RSI pressure pulsations are predicted from elementary fluid flow principles, and the calculated pressure mode shapes are shown to compare favorably with measured ones.

Model testing of hydro-machinery has long been used to assess expected prototype unsteady behavior. Pressure pulsation measurements in the spiral case, in the priming chamber between runner and wicket gates, and in the draft tube are commonly made. Other measurement locations may be employed for special situations or for research and development. Other unsteady measurements may also be made, such as forces and moments on the wicket gates or runner. Deducing the physical phenomena inducing unsteadiness and scaling the measured data to full scale conditions are ongoing challenges.

Unsteady pressure at a particular location may be the summation of numerous physical phenomena. For example, in the priming chamber, the instantaneous pressure could result from the superposition of the effects of a nearby runner blade interacting with a wicket gate. Other effects include runner blade to wicket gate interactions that occurred earlier and now have radiated to the same location, as well as from numerous reflections of these waves. Stochastic flow induced turbulence and fluid flow acoustic resonances caused by the coincidence of pulsation wavelengths with water passage dimensions inside the machine or external to the machine as well as a large variety of fluid-structure interactions need to be considered. Even pressures associated with test stand pumps may influence the results. In the past, it has been necessary to infer the fundamental source of the pressure pulsations from measured frequencies and knowledge of the frequencies of underlying physical principles. An additional tool in this process is the Operating Deflection Shape (ODS) technique, which permits visualization of complex temporal and spatial patterns. These patterns may then be compared to predictions, enabling a more direct evaluation of causation.

Rotor/Stator Interactions

Although RSI phenomena have been studied by others,[1] additional insight has been obtained from the following analysis. The RSI pressures must have a certain form to satisfy consistency and fluid physics. The consistency requirement of periodicity specifies the mathematical form of an integer number of cycles in one revolution. The fluid physics specifies that the magnitude of pressure on a blade depends on the flow field. These two concepts generate the form of the interaction of the pressure field on the runner and the flow field entering the runner. The pressure on the runner extends into the fluid and generates the pressure field away from the runner, such as is sensed between the runner and wicket gates.

The pressure field on the runner is required to be periodic with the number of blades. The form of the pressure, viewed from rotating coordinates, can be expressed as:

P (form of pressure on runner) = cos $(mZ_r\theta_r + \phi_m)$, where
m = an integer
Z_r = number of rotating blades
θ_r = angle coordinate on rotating runner
ϕ_m = phase angle for the mth harmonic

The value of m represents the harmonic of the pressure field. A value of $m = 0$ would represent a constant pressure, with no variation between buckets and plays no role in RSI. For $m = 1$, the pressure field would consist of one sinusoidal variation in pressure between each blade and would rotate with the runner. The runner pressure field would have the form of an infinite summation of these components, beginning with $m = 1$.

The actual magnitude of the pressure is a complicated function depending on both geometry and flow field. The magnitude of the pressure, therefore, remains unknown. The form of the flow field is known, as it must satisfy a periodic requirement related to the number of wicket gates. The flow field also has a harmonic content that may be expressed formally as:

Flow field from wicket gate = {Magnitude} cos $(nZ_s\theta + \phi_n)$, where: {Magnitude} represents an unknown value
n = an integer
Z_s = number of stationary vanes
θ = angle coordinate in stationary coordinates
ϕ_n = phase angle for the nth harmonic

The value of n represents the harmonic value of the flow field. A value of $n = 0$ would represent a constant flow, with no variation of velocity or angle between wicket gates. This value has meaning as the average value of wicket gate discharge. For $n = 1$, the pressure field would consist of one sinusoidal variation in flow field between each wicket gate. The wicket gate flow field would have the form of an infinite summation of these components, beginning with $n = 0$. Further considerations can be added to account for flow field variations related to the stay vanes or for the spiral case.

The pressure on the runner, or in the region of the runner, is the product of the magnitude of the flow field from the wicket gate and the form of the pressure on the runner. Formally, this may be expressed as:

$$P = A_{mn} \cos (nZ_s\theta + \phi_n) \cos (mZ_r\theta_r + \phi_m)$$

where A_{mn} is the amplitude of each harmonic contribution.[2] This form of the RSI pressure is inconvenient as it contains terms rotating with the runner and terms stationary with the wicket gates. The RSI pressure can be expressed in either rotating or stationary systems.

By using $\theta = \theta_r + \Omega t$, where Ω is the shaft rotational speed, t is time, and cosine relation cos (a) cos $(b) = 1/2[\cos (a + b) + \cos (a - b)]$, the pressure distribution, in stationary coordinates, becomes:

Based on a paper presented at the 11th International Meeting of the Work Group on the Behaviour of Hydraulic Machinery Under Steady Oscillatory Conditions, Stuttgart, Germany, October 8-10, 2003.

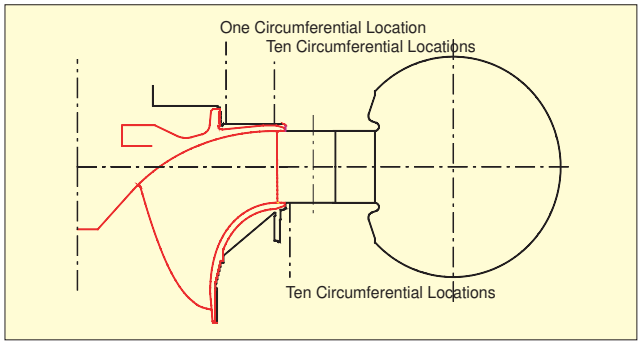

Figure 1. Pressure transducer radial locations.

$$P = A_{mn} \cos [mZ_r\Omega t - (mZ_r - nZ_s)\theta + \phi_m + \phi_n] + A_{mn} \cos [mZ_r\Omega t - (mZ_r + nZ_s)\theta + \phi_m - \phi_n]$$

This equation is the RSI pressure field as a function of space and time.[3] Two properties of this relationship are the characteristic pressure distributions (pressure mode shapes) having a number of spatial nodes, and the motion of the nodes. It is convenient to use the familiar diametral pressure mode number variable, $k = mZ_r \pm nZ_s$ (the diametral mode number variable has been long noted incorrectly in the literature as $\pm k = m\ Z_r - nZ_s$ but the correct form is $k = mZ_r \pm nZ_s$). Also note that the nodes rotate, that is have a spin speed (ss) in the stationary system with a frequency of $mZ_r\Omega/k$ .The first term yields the familiar, $k_1 = mZ_r - nZ_s$, having lower number of diametral nodes. The second term, $k_2 = mZ_r + nZ_s$, has a higher number of diametral nodes. The phase angle should be a single value for each n, m combination. A positive k value indicates that the diametral nodes rotate in the same direction as the runner, while negative values show counter rotation.

For the tested pump-turbine with 20 wicket gates, two runners were used, with six and nine blades, respectively. The frequencies and diametral mode numbers for each are tabulated in Tables 1 and 2.

Model Testing

A scale model pump turbine was instrumented and operated to determine RSI pressure shapes and frequencies. The instruments employed were flush mounted piezoresistive pressure transducers manufactured by PCB Piezotronics, Inc. Ten circumferential locations were instrumented in the priming chamber between the runner and wicket gates, as well as ten circumferential locations in the chamber between the runner and head cover. One transducer was located between the runner and head cover just outboard of the crown seal. Figure 1 shows the radial location of the pressure transducers.

Data Acquisition and Processing

Operating Deflection Shape (ODS) analysis is traditionally a technique whereby structural motions are measured using accelerometers. Accelerations are reduced to patterns of relative deformation and visualized through animated graphics. In this case, pressure transducers replace accelerometers resulting in visualization of time variant pressure distributions.

Data acquisition is performed by Dactron Inc.'s SpectraBook. Eight channels of pressure transducer time history data are simultaneously acquired, with one of the channels being maintained as a reference. Dactron's RTPro data acquisition software calculates, averages and saves Auto Power Spectra for each measurement channel, plus the Cross Power Spectra between all measurement channels and the maintained reference.

Saved Auto- and Cross-Power Spectra are imported by Vibrant Technology, Inc.'s ME'scopeVES modal software from which complex valued ODS Frequency Response Functions (ODS FRF) are calculated. As shown in Figure 2, each ODS FRF

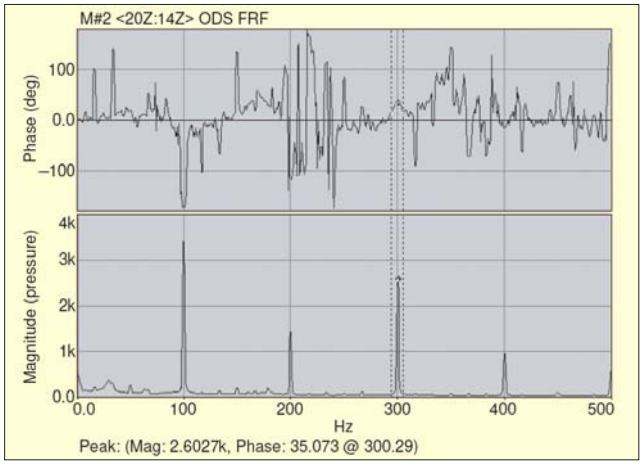

Figure 2. Typical complex valued pressure ODS FRF.

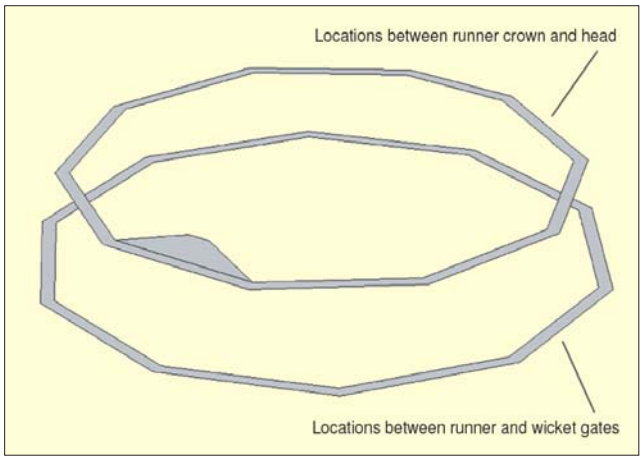

Figure 3. ODS pressure transducer geometry.

Table 1. RSI frequencies and diametral mode numbers for 6 runner blades and 20 wicket gates.

				Stationary		
n	m	k_1	k_2	ss1/Ω	ss2/Ω	Frequency/Ω
0	1	6	6	1	1	6
0	2	12	12	1	1	12
0	3	18	18	1	1	18
0	4	24	24	1	1	24
0	5	30	30	1	1	30
1	1	–14	26	–0.4	0.2	6
1	2	–8	32	–1.5	0.4	12
1	3	–2	38	–9.0	0.5	18
1	4	4	44	6.0	0.5	24
1	5	10	50	3.0	0.6	30
2	1	–34	46	–0.2	0.1	6
2	2	–28	52	–0.4	0.2	12
2	3	–22	58	–0.8	0.3	18
2	4	–16	64	–1.5	0.4	24
2	5	–10	70	–3.0	0.4	30

Table 2. RSI frequencies and diametral mode numbers for 9 runner blades and 20 wicket gates.

				Stationary		
n	m	k_1	k_2	ss1/Ω	ss2/Ω	Frequency/Ω
0	1	9	9	1	1	9
0	2	18	18	1	1	18
0	3	27	27	1	1	27
0	4	36	36	1	1	36
0	5	45	45	1	1	45
1	1	–11	29	–0.8	0.3	9
1	2	–2	38	–9.0	0.5	18
1	3	7	47	3.9	0.6	27
1	4	16	56	2.3	0.6	36
1	5	25	65	1.8	0.7	45
2	1	–31	49	–0.3	0.2	9
2	2	–22	58	–0.8	0.3	18
2	3	–13	67	–2.1	0.4	27
2	4	–4	76	–9.0	0.5	36
2	5	5	85	9.0	0.5	45

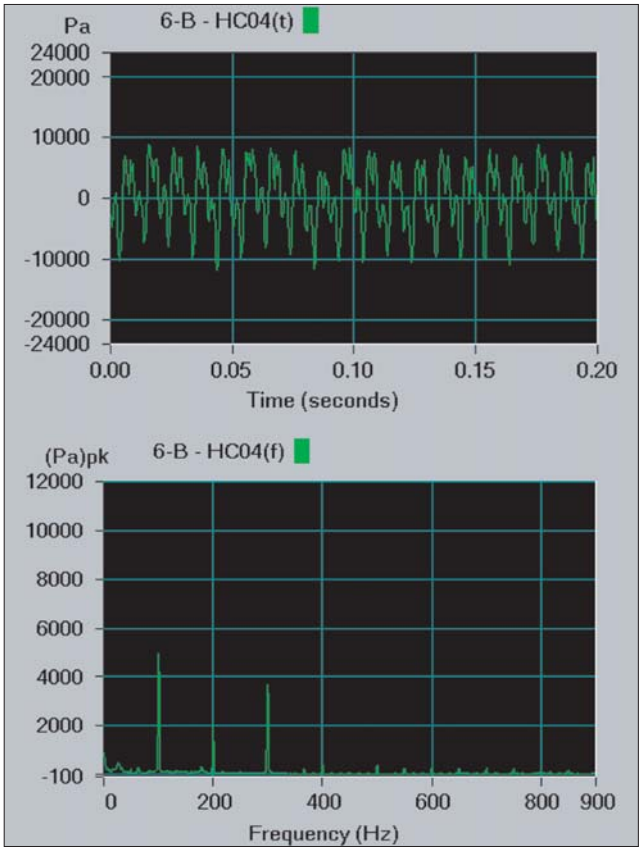

Figure 4. Six-bladed head cover pressure time history/spectrum.

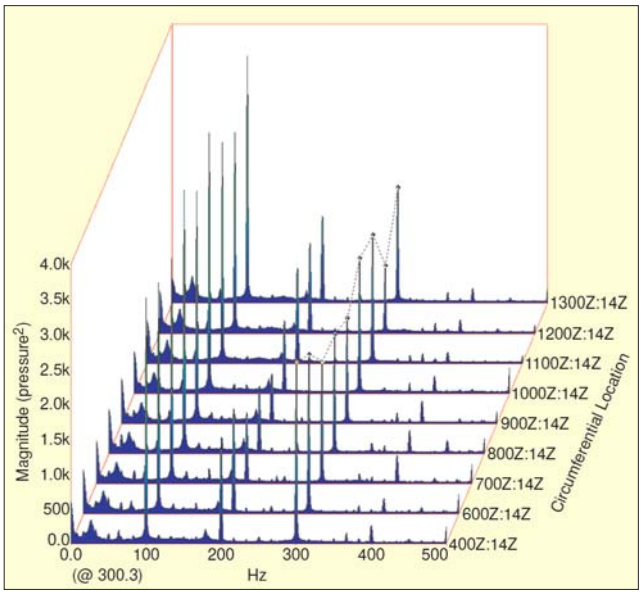

Figure 5. Six-bladed head cover waterfall plot.

possesses pressure magnitude and relative phase information. Geometry is established within ME'scopeVES. Figure 3 presents the represented pressure transducer locations. Each RSI

Table 3. Comparison of 6 bladed expected and tested pressure mode numbers and spin speed.

		Theory		Test		
n	m	k	ss/Ω	k	ss/Ω	f/Ω
0	1	6	1	NR	–	6
1	2	–8	–1.5	NR	–	12
1	3	–2	–9	–2	–9	18
1	4	4	4	4	6	24

NR = Not resolvable

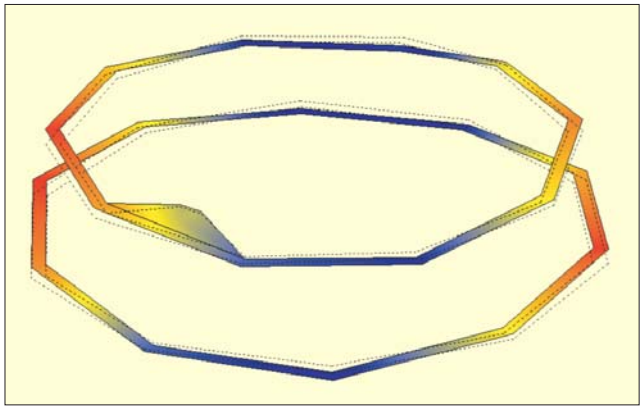

Figure 6a. Six-bladed runner pressure mode at 18 times rotational speed corresponding to n = 1, m = 3; showing k = –2.

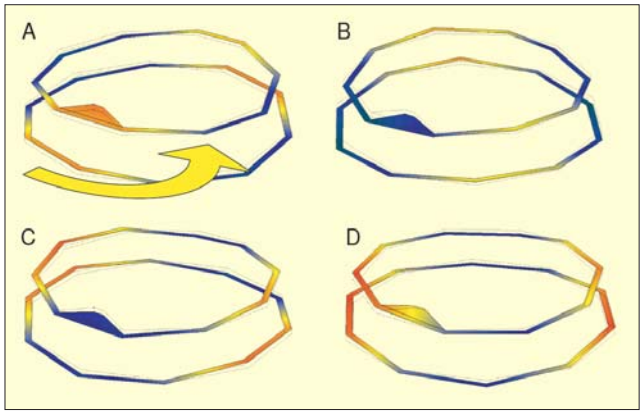

Figure 6b. Six-bladed, k = –2, CCW rotation demonstrating the spin speed in a series of images. Each image is 1/4 period of the pressure pulsation frequency (BPF period). The first image also shows the pattern after 2 periods, as the spin speed completes one revolution. A – t = 0.0 & t = 6.67 ms, (0) & (2) BPF periods. B – t = 0.83 ms, (1/4) BPF period. C – t = 1.67 ms, (1/2) BPF period. D – t = 2.5 ms, (3/4) BPF period.

forcing frequency possesses a global time variant pressure distribution.

By inspecting the frequency domain pressure signals, a number of dominant frequencies appear. By visualizing the pressure variation at the measurement locations at the frequency selected, a pressure characteristic shape (pressure mode shape) appears. Modal software correlates geometric transducer locations with their respective data blocks, allowing for animation of the pressure distribution.

The pump-turbine model was tested at 1000 rpm (Ω = 104.72 rad/s, f = 16.67 Hz) with a clockwise rotation. The spatial resolution of 10 transducers limits the number of diametral nodes which can be detected. Based on 10 transducers, one could expect that up to k = 4 may be resolvable. Additionally, the experiment was not designed to pick up diametral mode shapes having frequencies greater than f/Ω = 30.

Results

Six-Bladed Runner. Figure 4 presents a typical time history and frequency spectrum for a six-bladed head cover pressure transducer. A waterfall plot of all head cover pressure spectra

Table 4. Comparison of 9 bladed expected and tested pressure mode numbers and spin speed.

		Theory		Test		
n	m	k	ss/Ω	k	ss/Ω	f/Ω
0	1	9	1	NR	–	9
1	2	–2	–9	–2	–9	18
1	3	7	3.9	NR	–	27

NR = Not resolvable

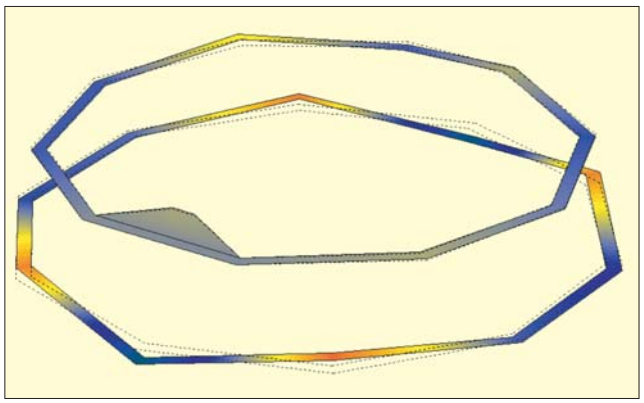

Figure 7a. Six-bladed runner pressure mode at 24 times rotational speed corresponding to n =1, m = 4; showing k = 4.

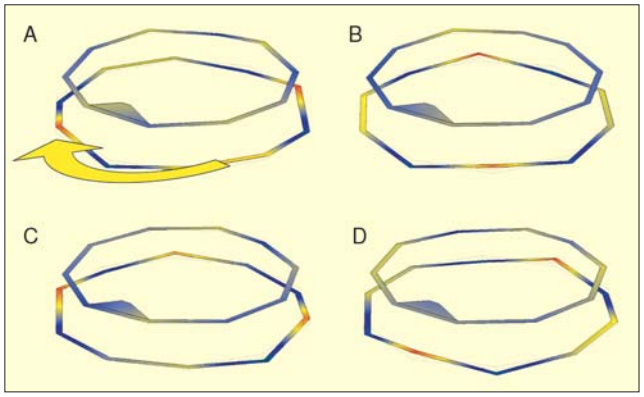

Figure 7b. Six-bladed, k = +4, CW rotation demonstrating the spin speed in a series of images. Each image is 1/5 period of the pressure pulsation frequency (BPF period). ***The first image also shows the pattern after 4 periods, as the spin speed completes one revolution.*** *A – t = 0.0 sec & t = 10.0ms, (0) & (4) BPF periods. B – t = 0.50 ms, (1/5) BPF period. C – t = 1.0 ms, (2/5) BPF period. D – t = 1.5 ms, (3/5) BPF period.*

is presented for information in Figure 5.

For the six-bladed runner, the lowest RSI calculated diametral mode number in Table 1 occurs with $n = 1$ and $m = 3$ to give $k = -2$ at a frequency of $3 \times 6 \times \Omega$. For $k = -2$, the spin speed is $[3 \times 6/(-2)]\ \Omega$. For the 1000 rpm test speed, $3 \times 6 \times \Omega = 300$ Hz. Figure 6a presents a graphic of the six-bladed pressure distribution that occurs at 300 Hz (18× runner speed) and shows a clear $k = 2$ pattern. The series of graphics in Figure 6b shows that this pattern rotates in a counter clockwise direction (opposite from runner rotation) and is therefore $k = -2$. The expected spin speed of $[3 \times 6/(-2)]\ \Omega = -9\ \Omega$ (150 Hz) is also confirmed. At the same frequency, $k = 38$ is also expected, but cannot be resolved with 10 circumferential transducers.

The next highest calculated diametral mode number in Table 1 occurs with $n = 1$ and $m = 4$ gives $k = +4$ at a frequency of $4 \times 6 \times \Omega$. For the 1000 rpm test speed, $4 \times 6 \times \Omega = 400$ Hz. Figure 7a presents a graphic of the six-bladed pressure distribution that occurs at 400 Hz (24× runner speed) and shows a clear $k = 4$ pattern. The series of graphics in Figure 7b shows that the $k = +4$ shape rotates in a clockwise direction (coincident with runner rotation). The expected spin speed of $[4 \times 6/(4)]\ \Omega = 6\ \Omega$ (100 Hz) is also confirmed. At the same frequency, $k = 44$ is also expected, but cannot be resolved with 10 circumferential transducers.

Based on inspection of the data, all low k number pressure mode shapes were found. A number of $k = 0$ and $k = 1$ mode shapes thought to be associated with the model or model test stand were also identified. Pressure mode shapes associated with higher than $n = 1$ inflow field periodic number seem to be of significantly lower magnitude. Table 3 summarizes the observations.

Nine-Bladed Runner. Figure 8 presents pressure between runner crown and head cover time history and frequency spectrum for the nine-bladed test. A waterfall plot of all locations between runner crown and head cover nine-bladed pressure spectra is presented for information in Figure 9. For the nine-bladed runner, the lowest diametral mode number from Table 2 occurs with $n = 1$ and $m = 2$ to give $k = -2$ and $k = 38$ at a frequency of $2 \times 9 \times \Omega$. For $k = -2$, the spin speed is $[2 \times 9/(-2)]\Omega$. For a test speed of 1000 rpm, $2 \times 9 \times \Omega = 300$ Hz.

Figure 10a presents a graphic of the nine-bladed $k = -2$ pressure distribution that occurs at 300 Hz (18× runner speed). The series of graphics in Figure 10b shows that the $k = -2$ shape rotates in a counter clockwise direction (opposite from runner rotation). The expected spin speed of $[2 \times 9/(-2)]\ \Omega = -9\Omega$ (150 Hz) is also confirmed.

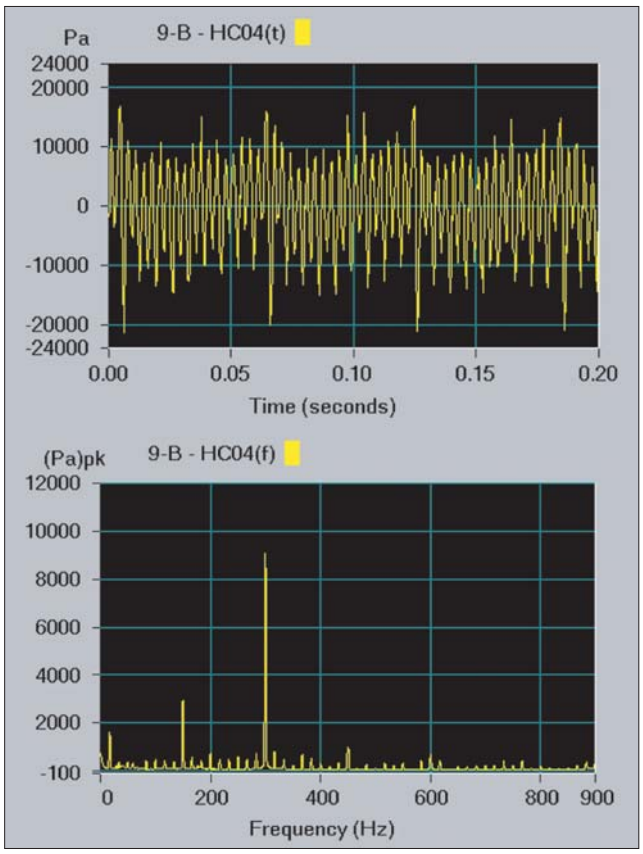

Figure 8. Nine-bladed pressure between runner crown and head cover time history/spectrum.

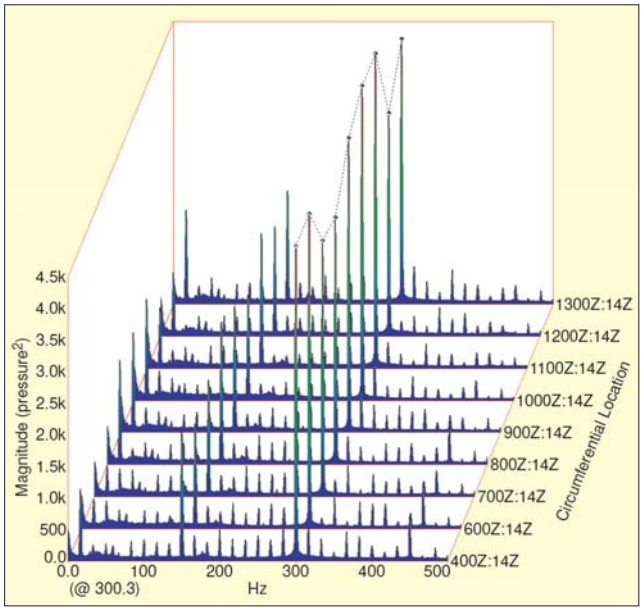

Figure 9. Nine-bladed head cover waterfall plot.

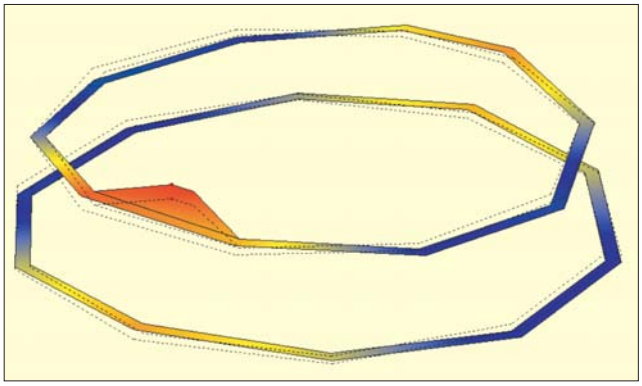

Figure 10a. Nine-bladed runner pressure mode at 18 times rotational speed corresponding to n = 1, m = 2; showing k = –2.

The next highest diametral mode number occurs with m = 3 and $n = 1$ gives $k = +7$ at a frequency of $3 \times 9 \times \Omega$ Hz. At this frequency, 7 diametral nodes would require significantly more than 10 transducers to spatially resolve the waveform. Therefore, in contrast to the six-bladed runner, this diametral mode number cannot be visualized with the current experimental setup, but it was confirmed by data analysis beyond the scope of this article.

Based on inspection of the data, all low k number pressure mode shapes were found. A number of $k = 0$ and $k = 1$ mode shapes thought to be associated with the model were also identified. Table 4 summarizes the observations.

Summary

A re-look at the RSI equations has provided additional insight related to pressure mode shapes. Higher mode numbers not previously discussed in the literature were presented.

The ODS method has been used with model testing to visualize some RSI pressure mode shapes in the priming chamber and in the chamber between the runner crown and headcover. These time variant pressure distributions agree with expected patterns from the RSI equations.

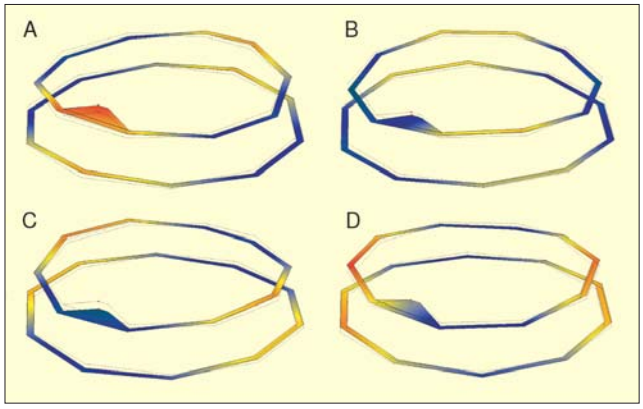

Figure 10b. Nine-bladed, k = –2, CCW rotation demonstrating the spin speed. Each image is 1/4 period of the pressure pulsation frequency (BPF period). The first image also shows the pattern after two periods, as the spin speed is half of the m = 2 frequency. A – t = 0.0 & t = 6.67 ms (0) & (2) BPF periods. B – t = 0.83 ms. (1/4) BPF period. C – t = 1.67 ms (1/2) BPF period. D – t = 2.5 ms, (3/4) BPF period.

References

1. Tanaka, H., "Vibration Behaviour and Dynamic Stress of Runners of Very High Head Reversible Pump-Turbines." IAHR Symposium, Belgrade, 1990, Section U2.
2. Dubas, M. "Uber die Erregung infolge der Periodizitat von Turbomachinen." Ingenieur-Archiv 54, 1984, pp. 413-426.
3. Blake, W., *Mechanics of Flow-Induced Sound and Vibration*, Vol. II, Academic Press, Inc., 1986, ISBN 0-12-103502-6 (v. 2), p. 916. SV

The authors can be contacted at: cpowell@StructuralTechnology.com.